Decomposition Mechanisms of Trivinylantimony and Reactions with Trimethylgallium

Cory A. Larsen,[†,‡] Robert W. Gedridge, Jr.,*[,§] and Gerald B. Stringfellow[†]

Department of Materials Science and Engineering, University of Utah, Salt Lake City, Utah 84112, and Chemistry Division, Research Department, Naval Weapons Center, China Lake, California 93555-6001

Received May 18, 1990. Revised Manuscript Received October 1, 1990

The decomposition of trivinylantimony (TVSb) was studied in an atmospheric pressure flow tube reactor, with D_2 and He as carrier gases. The products were analyzed by a time-of-flight mass spectrometer. TVSb pyrolyzes at similar temperatures in D_2 and He by either gas-phase homolytic fission of the Sb–C bonds to form CH_2=CH radicals or by an Sb-centered reductive elimination pathway. D radicals, produced from interactions between CH_2=CH and/or CH_3 (from trimethylgallium (TMGa)) with a D_2 ambient, do not appear to enhance the pyrolysis of TVSb. Addition of azomethane ($(CH_3N)_2$) as a source of methyl radicals enhances the pyrolysis of TVSb in He. The addition of TMGa lowers the decomposition temperature of TVSb in D_2 by providing a source of methyl radicals. There are competing homogeneous and heterogeneous components in the decomposition of TMGa–TVSb mixtures. The decomposition of TVSb alone or in a 1:1 ratio with TMGa results in heavy carbonaceous deposits in the reactor. Decreasing the V/III ratio to 0.53 eliminates these deposits.

Introduction

As organometallic vapor-phase epitaxy (OMVPE) progresses from a novel to a mature technique for producing III/V semiconductors, one of the areas of research with obvious benefits is the design and development of new source compounds. Great strides have been made with *tert*-butylarsine (TBAs) and *tert*-butylphosphine (TBP),[1,2] respectively, as replacements for AsH_3 and PH_3. These source compounds were unknown until a few years ago. There are two main reasons for investigating new source compounds. The first is to find precursors that are safer to handle than the "conventional" compounds like AsH_3 and PH_3. The second reason is to alter the chemistry to obtain desired properties such as low pyrolysis temperature and reduction of carbon incorporation in layers grown by OMVPE.

Development of new Sb sources is of interest for several reasons having to do with the unique properties of Sb-containing semiconductors. Many of these materials melt at low temperatures (525 °C for InSb, as compared to 1240 °C for GaAs). A source compound with a low pyrolysis temperature is needed if sharp interfaces and small features are to be obtained. In the case of materials containing both Sb and Bi, the situation is further complicated by the tendency of Bi to phase separate.[3] Therefore, low growth temperatures are required to limit the formation of a second liquid phase in these alloys.

Trimethylantimony (TMSb) is almost universally used at present. It pyrolyzes at approximately 450 °C, depending on the ambient gas.[4] One way to lower the decomposition temperatures is to use compounds with Sb–H bonds. Recently SbH_3 was used successfully to grow InSb at 300 °C.[5] However, SbH_3 as well as the higher homologues CH_3SbH_2 and $(CH_3)_2SbH$ are so unstable that room-temperature storage is impossible.[6,7] In the case of InSb growth with SbH_3, the Sb source compound was generated at the point of use.

It was felt that trivinylantimony (TVSb) might be an acceptable alternative to TMSb. The vapor pressure of TVSb is approximately 8.5 Torr at room temperature,[8] which is in the acceptable range for OMVPE sources. Another motivation for studying TVSb is that tetravinyletllurium(IV) (TVTe) is unexpectedly less stable than tetramethyltellurium(IV) (TMTe).[9] If TVTe decomposes by a free-radical pathway as does TMTe, one would expect greater stability for TVTe based on the higher activation energy for vinyl radical formation in comparison to methyl radical formation.[10] However, TVTe thermally and photolytically decomposes, in excess 1,4-cyclohexadiene as a free-radical trapping reagent, according to eq 1.[11]

$$(CH_2{=}CH)_4Te \rightarrow (CH_2{=}CH)_2Te + HC{\equiv}CH + CH_2{=}CH_2 \quad (1)$$

$HC{\equiv}CH$ and $CH_2{=}CH_2$ were produced in a 1:1 ratio. The formation of $HC{\equiv}CH$ in the presence of a free-radical trapping reagent suggested that TVTe decomposition was not free radical in nature. It was proposed that TVTe decomposition occurs by a noncoupling reductive elimination pathway.[11] This alternative pathway permits TVTe to decompose at temperatures lower than for TMTe. It was predicted that other organometallic compounds such as TVSb could exhibit similar behavior.

Experimental Section

Apparatus. The atmospheric pressure flow tube reactor used in these experiments has been described in detail elsewhere.[12] The

[†] University of Utah.

[‡] Current address: Department of Electronic Materials Engineering, Australian National University, GPO Box 4, Canberra, ACT, 2601.

[§] Naval Weapons Center.

(1) Haacke, G.; Watkins, S. P.; Burkhard, H. *Appl. Phys. Lett.* **1989**, *54*, 2029.
(2) Kurtz, S. K.; Olson, J. M.; Kibbler, A. *J. Electron. Mater.* **1989**, *18*, 15.
(3) Ma, K. Y.; Fang, Z. M.; Jaw, D. H.; Cohen, R. M.; Stringfellow, G. B. *Appl. Phys. Lett.* **1989**, *55*, 2420.
(4) Larsen, C. A.; Li, S. H.; Stringfellow, G. B. *Chem. Mater.*, in press.
(5) Sugiura, O.; Kameda, H.; Shiina, K.; Matsumura, M. *J. Electron. Mater.* **1988**, *17*, 11.
(6) Devyatykh, G. G.; Kedyarkin, V. M.; Zorin, A. D. *Russ. J. Inorg. Chem.* **1969**, *14*, 1055.
(7) Burg, A. B.; Grant, L. R. *J. Am. Chem. Soc.* **1959**, *81*, 1.
(8) Maier, L.; Seyferth, D.; Stone, F. G. A.; Rochow, E. G. *J. Am. Chem. Soc.* **1957**, *79*, 5884.
(9) Gedridge, Jr., R. W.; Harris, D. C.; Higa, K. T.; Nissan, R. A. *Organometallics* **1989**, *8*, 2817.
(10) (a) Hoke, W. E.; Lemonias, P. J.; Korenstein, R. *J. Mater. Res.* **1988**, *3*, 329. (b) *Handbook of Chemistry and Physics*, 70th ed.; Weast, R. C., Ed.; CRC Press: Boca Raton, FL, 1988; pp F206–207.
(11) Gedridge, Jr., R. W.; Higa, K. T.; Nissan, R. A. *Organometallics*, in press.

0897-4756/91/2803-0096$02.50/0

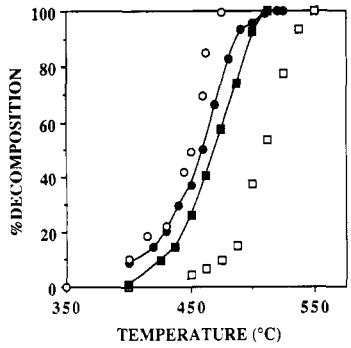

Figure 1. Pyrolysis of 0.9% TVSb in He (■) and D_2 (●) and 1.0% TMSb in He (□) and D_2 (○) vs temperature.

use of D_2 instead of H_2 as a carrier gas allows the pyrolysis products to be isotopically labeled. The carrier gases pass through mass flow controllers and then through stainless steel bubblers containing the reactants. The gas mixture enters the reactor, which is a quartz tube of 4-mm i.d. and a hot zone 41.5 cm long. The exhaust gases are sampled continuously via a variable leak connected to a CVC 2000 time-of-flight mass spectrometer. The m/z = 148 peak intensity was monitored for determination of the percent decomposition of TVSb. The flow rate for most experiments was 40 sccm. The TVSb concentration for most experiments was 0.9%. In each case, the reactor was conditioned by heating the tube to a temperature near which 50% of the TVSb decomposed. For some runs the tube was packed with SiO_2 chips to increase the surface area approximately 24 times. The flow rates were correspondingly adjusted to give the same residence times as for the unpacked runs.

General Synthetic Procedures. Organic solvents were distilled under Ar from sodium/benzophenone. Synthesis was carried out under purified Ar using Schlenk techniques.[13] Air- and moisture-sensitive materials were transferred inside a He-filled Vacuum Atmospheres glovebox. TVSb was prepared from the reaction of $SbCl_3$ (99.999%) with vinylmagnesium bromide in tetrahydrofuran.[8] The distilled water used for the aqueous workup was freeze–thaw degassed prior to use. The organic layer containing TVSb was dried over anhydrous $MgSO_4$ for 24 h. The colorless liquid was collected and purified three times by vacuum distillation (55–56 °C at 29–30 Torr). ^1H and ^{13}C NMR spectra were consistent with the literature.[14]

The azomethane was synthesized by the method of Foster and Beauchamp[15] using 1,2-dimethylhydrazine dihydrochloride purchased from Aldrich Chemical Co. The D_2 was research grade (to minimize background HD levels), from Air Products and Chemicals, Inc.

Results

Pyrolysis of TVSb Alone. Figure 1 shows the percent decomposition of TVSb as a function of temperature in He and D_2. As a comparison, the pyrolysis of TMSb is included. A change of the carrier gas alters the decomposition rate of TVSb only slightly. The temperature difference of 10 °C is close to the error limits of the system. Thus these ambient gases do not play a major role in TVSb pyrolysis. By contrast, replacing He with D_2 lowers the reaction temperature of TMSb by over 50 °C.[4]

The similarity of the reaction in the two carriers implies indirectly that the process is unimolecular in both. The validity of the first-order hypothesis can be tested in terms of the integrated rate law, given by

$$-\ln [P/P_0] = kt \qquad (2)$$

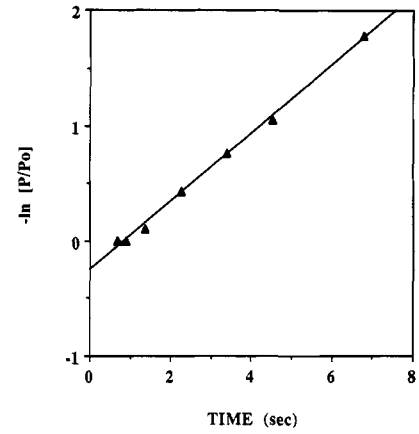

Figure 2. Plot of $-\ln [P/P_0]$ vs residence time in the reactor at 475 °C.

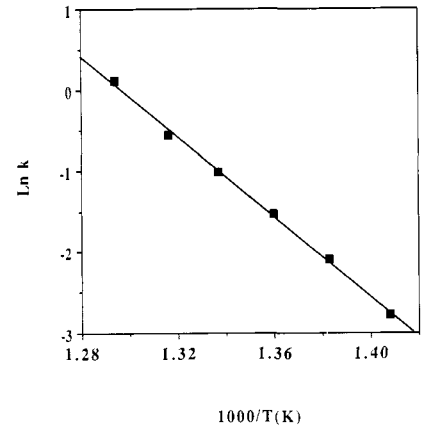

Figure 3. Arrhenius plot from the decomposition curve of TVSb in He at low surface area.

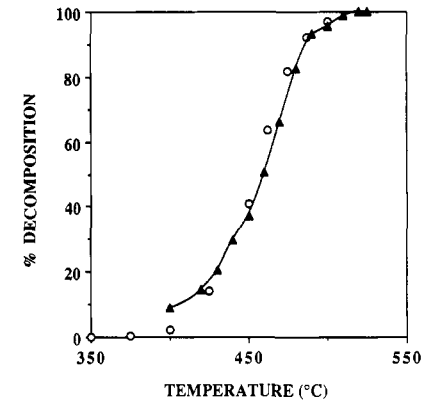

Figure 4. Pyrolysis of 0.9% TVSb in D_2 with low (▲) and high (○) surface areas.

where P and P_0 are the final and initial pressures, and t is the residence time in the reactor. The pressures were not directly measured. Instead, the intensities of the TVSb mass spectral peaks (m/z = 148), which are proportional to the pressures, were used. If the first-order assumption is correct, a plot of $-\ln [P/P_0]$ versus t should give a straight line passing through the origin. As shown in Figure 2, this assumption is nearly correct. Therefore, pyrolysis data in He can be used to calculate P/P_0 for the entire temperature range, and the results used to construct an Arrhenius plot as indicated in Figure 3. The resulting rate constant is

$$\log k\ (s^{-1}) = 13.88\text{–}49.00\ (\text{kcal/mol})/2.303RT \qquad (3)$$

The activation energy for TVSb decomposition derived

(12) Buchan, N. I.; Larsen, C. A.; Stringfellow, G. B. *Appl. Phys. Lett.* **1987**, *51*, 1024.
(13) Shriver, D. F.; Drezdzon, M. A. *The Manipulations of Air-Sensitive Compounds*, 2nd ed.; Wiley: New York, 1986.
(14) Ashe, III, A. J.; Ludwig, Jr., E. G.; Pommerening, H. *Organometallics* **1983**, *2*, 1573.
(15) Foster, M. S.; Beauchamp, J. L. *J. Am. Chem. Soc.* **1972**, *94*, 2425.

Scheme I

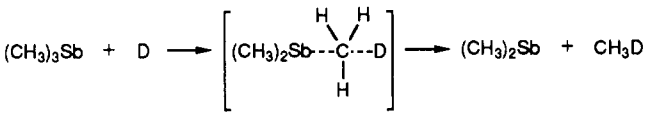

from eq 3 (49.00 kcal/mol) is less than the reported Sb–C bond energy for TMSb (55.9 kcal/mol).[16]

As a final experiment on TVSb alone, the surface area of the reactor was increased to determine the extent of heterogeneous pyrolysis reactions. As shown in Figure 4, a 24-fold increase in surface area did not affect the decomposition temperatures. Again, this is different from TMSb, for which a small surface component of the process was detected.

Proposed Mechanisms. Two alternative mechanisms for TVSb pyrolysis are proposed. At this stage the data are insufficient to completely define the pyrolysis mechanism. The first is simple Sb–C bond homolysis of TVSb to produce vinyl radicals. The expected subsequent radical reactions are

$$CH_2{=}CH + D_2 \rightarrow CH_2{=}CHD + D \quad (4)$$

$$CH_2{=}CH + D \rightarrow CH_2{=}CHD \quad (5)$$

$$2CH_2{=}CH \rightarrow CH_2{=}CHCH{=}CH_2 \quad (6)$$

$$2CH_2{=}CH \rightarrow CH_2{=}CH_2 + HC{\equiv}CH \quad (7)$$

Step 4 would create a large number of D atoms. This can be shown by comparing the rates for the analogous reactions in H_2 for vinyl and methyl radicals. The rate constant for the reaction

$$CH_2{=}CH + H_2 \rightarrow CH_2{=}CH_2 + H \quad (8)$$

is reported as[17]

$$\log k_8\ (\text{L/mol s}) = 9.9 - 7.4\ (\text{kcal/mol})/2.303RT \quad (9)$$

whereas for methyl radicals, i.e.

$$CH_3 + H_2 \rightarrow CH_4 + H \quad (10)$$

the rate is[18]

$$\log k_{10}\ (\text{L/mol s}) = 8.93 - 10.9\ (\text{kcal/mol})/2.303RT \quad (11)$$

At a representative temperature of 450 °C, $k_8/k_{10} = 114$. It was shown that the acceleration of TMSb decomposition in D_2 was due to D atom attack on the parent molecule.[4] If D atoms are produced during TVSb pyrolysis, they do not have an effect on the rate.

The difference in pyrolysis behavior for the two Sb compounds in D_2 may be attributed to the mode of attack of the D atoms. The D–Sb bond is very weak and hence attack on the central atom is unlikely. In the case of TMSb, the D atoms probably approach the CH_3 ligands from the side opposite the Sb–C bond in an S_N2 transition state (Scheme I). Hydrogenolysis of TMSb via a pentacoordinate Sb(V) intermediate can be ruled out since this type of Sb(V) hydride is unknown. The formation of a Sb(V) hydride is not thermodynamically favorable in comparison to the analogous intermediate of TMAs,[4] which does decompose by hydrogenolysis. In contrast, D attack on the central atom in $(CH_3)_3As$ is favorable such that significant amounts of $(CH_3)_2AsD$ are found in the pyrolysis of $(CH_3)_3As$.[19]

The other possible mechanism for TVSb pyrolysis involves Sb-centered reductive elimination pathways:

$$(CH_2{=}CH)_3Sb \rightarrow (CH_2{=}CH)Sb + CH_2{=}CHCH{=}CH_2 \quad (12)$$

$$(CH_2{=}CH)Sb \rightarrow CH_2{=}CH + Sb \quad (13)$$

$$(CH_2{=}CH)Sb + D_2 \rightarrow (CH_2{=}CH)SbD_2 \quad (14)$$

$$(CH_2{=}CH)SbD_2 \rightarrow CH_2{=}CHD + SbD \quad (15)$$

$$SbD \rightarrow Sb + D \quad (16)$$

This route would generate $CH_2{=}CHCH{=}CH_2$ in the first step by coupling two vinyl groups (eq 12). There are several reasons for suspecting this to be the operative mechanism. First, the activation energy for TVSb decomposition (eq 3) is less than that found for scission of the Sb–CH_3 bond in TMSb.[4,16] If Sb–C bond homolysis occurs, one would expect the Sb–vinyl bond strength to be higher than the Sb–methyl bond strength. Second, TVSb decomposes 50 °C lower as compared to TMSb in He. These observations are contrary to the predicted higher activation energy for vinyl radical formation in comparison to methyl radical formation. This implies that the rate-determining step in TVSb decomposition may not involve Sb–C bond homolysis to form vinyl radicals. However, one cannot rule out the possibility of the $(CH_2{=}CH)Sb$ intermediate decomposing to $CH_2{=}CH$ radicals (eq 13).

Another consideration in elucidating the TVSb pyrolysis mechanism is the identification of the byproducts. In He, as in D_2, the products in these experiments include a variety of unsaturated hydrocarbons, including long-chain hydrocarbons (1,3,5-hexatriene) from oligomerization reactions involving the alkene byproducts. Quantitative determinations or even unambiguous identifications of these byproducts are difficult. Nevertheless, some useful information can be derived. In D_2, the only products observed were $CH_2{=}CHD$ and $CH_2{=}CHCH{=}CH_2$. It was not possible to determine the $CH_2{=}CH_2$ concentration due to the overlap of its spectrum with the fragments of other molecules. $HC{\equiv}CH$ was not detected, indicating that the noncoupling reductive elimination pathway observed from the TVTe study[11] is not operative for this molecule. Furthermore, if vinyl radicals are present, they should disproportionate as well as recombine (eqs 6 and 7). The nonproduction of vinyl radicals is further attested by an experiment in which a high concentration of C_7D_8 (C_7D_8/TVSb = 5/1) was added to TVSb in He. In this case, no $CH_2{=}CHD$ was found. This implies vinyl radicals are not present or C_7D_8 is not an effective vinyl radical trapping reagent.

While the reductive elimination reaction in eq 15 would result in the formation of $CH_2{=}CHD$, the formation of deuterated Sb intermediates is not expected at elevated temperatures due to their predicted instability even at room temperature. If these intermediates do form, they are short lived and were not detected by the mass spectrometer.

In summary, the data are inconclusive in determining whether the thermal decomposition of TVSb is a simple case of gas-phase homolytic scission of the Sb–C bonds to form vinyl radicals, Sb-centered reductive elimination pathways, or some combination of these reactions. However, experimental evidence suggests that the most likely

(16) Price, S. J. C.; Richard, J. P. *Can. J. Chem.* **1972**, *50*, 966.
(17) *CRC Handbook of Bimolecular and Termolecular Gas Reactions*; Kerr, J. A., Moss, S. J., Eds.; CRC Press: Boca Raton, FL, 1981; p 301.
(18) Kerr, J. A.; Parsonage, M. J. *Evaluated Kinetic Data on Gas Phase Hydrogen Transfer Reactions of Methyl Radicals*; Butterworths: London, 1976; p 26.
(19) Li, S. H.; Larsen, C. A.; Stringfellow, G. B. *J. Cryst. Growth* **1990**, *102*, 117.

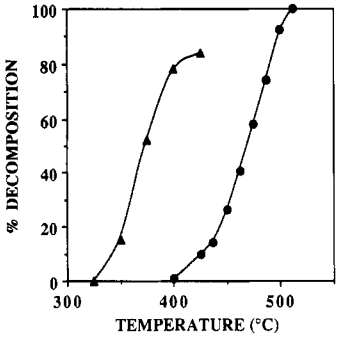

Figure 5. Pyrolysis of 0.9% TVSb in He (●) and with 4.6% azomethane (▲).

pyrolysis reaction involves an Sb-centered reductive elimination pathway. Neither vinyl radicals nor any subsequent reaction products appear to influence the parent molecules. Rather, they are removed by the usual gas-phase reactions.

Reaction of TVSb with TMGa. The next step in the study was to investigate the effects of a group III precursor in order to simulate the conditions of OMVPE growth. The situation is potentially quite complex. Nevertheless, some important features were identified. The first experiment was to determine the effect of methyl radicals on TVSb pyrolysis, since most group III precursors used for OMVPE are trimethyl compounds. The methyl radical source used was azomethane, $(CH_3N)_2$. This compound has the advantage of being a "clean" radical source that decomposes at approximately 400 °C to give methyl radicals and N_2.[20] The concentrations of azomethane and TVSb were 4.6 and 0.9%, respectively. The carrier gas was He, to avoid any complications from the ambient gas. The results are shown in Figure 5, with the data from Figure 1 in He for comparison. The addition of azomethane enhances the pyrolysis of TVSb. This suggests that methyl radicals attack the parent TVSb molecule. The thermodynamic driving force of the process may be large, since the CH_2=CH—Sb and CH_2=CH—CH_3 bond strengths differ by 50 kcal/mol.[21] The increased pyrolysis with added CH_3 may be due to attack of the methyls at the C_α to the Sb. The products are even more complex than for TVSb alone in He. They include those mentioned above as well as propene.

Next TMGa (0.7%) was added to TVSb (0.8%), at both high and low surface areas. Figure 6 shows the behavior of TVSb and TMGa. For the low surface area TVSb pyrolysis is shifted by approximately 50 °C to lower temperatures and the curve is monotonic. At the high surface area TVSb pyrolysis is shifted to significantly lower temperatures, but at approximately 410 °C the curves intersect. For TMGa, a somewhat reversed pattern is observed. At the low surface area there is a shoulder at 430 °C, above which point the pyrolysis approaches and intersects the curve for TMGa alone in D_2. At the high surface area the entire curve is shifted to lower temperatures.

For both compounds at the high surface area, the shoulders appear at similar temperatures to those at which the homogeneous gas-phase processes become important. This gives the main clue to what is going on. For each component there are homogeneous and heterogeneous parts to the decomposition. The main role of TMGa is to

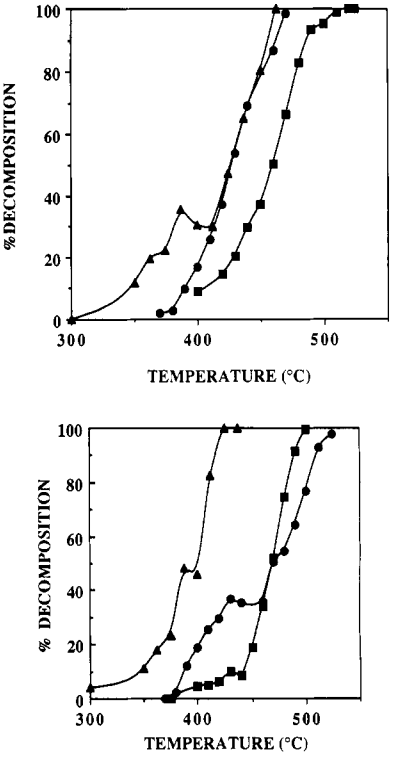

Figure 6. Top: Pyrolysis of 0.8% TVSb in D_2 alone (■) and with 0.7% TMGa at low (●) and high (▲) surface area. Bottom: Pyrolysis of 0.7% TMGa in D_2 alone (■) and with 0.8% TVSb at low (●) and high (▲) surface area.

supply CH_3 radicals, which react as discussed above. It is possible to pack the tube such that the surface reaction becomes noticeable, but at around 410 °C the homogeneous gas-phase processes take over. Simultaneously, the surface catalysis of TMGa decomposition is permitted for the low surface area, but again at 430 °C its homogeneous reactions take over. If the surface area is high enough, however, the heterogeneous reactions can be made to dominate, giving the curve farthest to the left in Figure 6, bottom. It should be noted that the enhancement of TVSb pyrolysis at low surface area is accompanied by a decrease in TMGa decomposition. For TMGa, the cleaved CH_3 radicals are quite important in the pyrolysis mechanism.[22] Hence these data offer further evidence that gas-phase methyl radicals enhance TVSb decomposition. The products offer more evidence that gas-phase reactions are taking place. At 450 °C, they include all the products found in the azomethane study and CH_3D from homogeneous TMGa pyrolysis.

Surface Composition. The final topic to be discussed is the nature of the surface in these experiments. For TVSb alone, the reactor tubes became coated with heavy deposits of black carbonaceous material, much heavier than for TMSb. The reaction pathways involving vinyl radicals make it likely that oligomers (as mentioned above, 1,3,5-hexatriene was found in the He experiments), polymers, and their decomposition products result in this deposit. Addition of TMGa in the above experiments did not remove this deposit. In contrast, addition of TMIn removed the carbonaceous solids in the pyrolysis of TMSb. Hence it is not accurate to speak of the surface reactions as occurring on GaSb. However, when the TMGa concentration was increased to 1.5%, giving a V/III ratio of 0.53, the solid product completely dissolved in aqua regia.

(20) (a) Page, M.; Pritchard, H. O.; Trotman-Dickenson, A. F. *J. Chem. Soc.* **1953**, 3878. (b) Foster, W.; Rice, O. K. *Can. J. Chem.* **1963**, *41*, 562.

(21) Benson, S. W. *Thermochemical Kinetics*, 2nd ed.; Wiley-Interscience: New York, 1976; p 309.

(22) Larsen, C. A.; Buchan, N. I.; Li, S. H.; Stringfellow, G. B. *J. Cryst. Growth* **1990**, *102*, 103.

Presumably it was some GaSb–Ga mixture.

Summary

The pyrolysis of TVSb has been investigated in a flow tube reactor using D_2 and He carrier gases. For TVSb alone, the most likely pyrolysis reaction involves an Sb-centered reductive elimination pathway. A less likely possibility is pyrolysis via homolysis of the Sb–C bonds, yielding vinyl radicals. Unfortunately, examination of the organic byproducts in both He and D_2 yields insufficient information to form a definitive hypothesis. However, in He the pyrolysis rate for TVSb is more rapid than for TMSb. Since vinyl radicals form stronger bonds than methyl radicals, this datum contradicts the Sb–C bond homolysis mechanism. Again, the activation energy for pyrolysis is less than the expected Sb–vinyl bond strength. Finally, the addition of C_7D_8 produces no CH_2=CHD, indicative of the absence of vinyl radicals. To elucidate our understanding of GaSb growth by using TMGa and TVSb, the pyrolysis rates for this combination of reactants were also studied. CH_3 radicals from $(CH_3N)_2$ pyrolysis were found to enhance TVSb pyrolysis in He. TMGa also increases the TVSb pyrolysis rate, mainly due to the methyl radicals produced. A heterogeneous pyrolysis reaction appears at high surface area. At V/III ratios normally used for OMVPE growth, carbonaceous deposits were formed. Thus, TVSb may be a useful precursor for OMVPE only at V/III ratios less than unity.

Acknowledgment. We acknowledge financial support from the Office of Naval Research, the Office of Naval Technology, and the Air Force Office of Scientific Research.

Registry No. TVSb, 5613-68-3; TMGa, 1445-79-0.

Structural Chemistry and Raman Spectra of Niobium Oxides

Jih-Mirn Jehng and Israel E. Wachs*

Zettlemoyer Center for Surface Studies, Department of Chemical Engineering, Lehigh University, Bethlehem, Pennsylvania 18015

Received May 29, 1990. Revised Manuscript Received November 5, 1990

A series of niobium oxide reference compounds were investigated by Raman spectroscopy in order to determine the relationship between niobium oxide structures and their corresponding Raman spectra. The assignments of the Raman bands were based on the known niobium oxide structures. The Raman studies indicate that the Raman frequencies strongly depend on the niobium oxide structures. For the slightly distorted octahedral NbO_6 structures ($KNbO_3$, $NaNbO_3$, and $LiNbO_3$), the major Raman frequencies appear in the 500–700-cm^{-1} region. For the highly distorted octahedral NbO_6 structures ($K_8Nb_6O_{19}$, $AlNbO_4$, and $Nb(HC_2O_4)_5$), the major Raman frequencies shift from the 500–700- to the 850–1000-cm^{-1} region. The distortions in the niobium oxide compounds are caused by the corner- or edge-shared NbO_6 octahedra. Both slightly distorted and highly distorted octahedral NbO_6 sites coexist in the $KCa_2Na_{n-3}Nb_nO_{3n+1}$, n = 3–5, layered compounds. Most of the niobium oxide compounds possess an octahedrally coordinated NbO_6 structure with different extents of distortion, and only a few rare-earth $ANbO_4$ (A = Y, Yb, Sm, and La) compounds possess a tetrahedrally coordinated NbO_4 structure. For the tetrahedral NbO_4 structure of $YbNbO_4$ the major Raman frequency appears at ~813 cm^{-1}. In situ Raman studies assisted in the discrimination between bulk and surface functionalities in the niobium oxide reference compounds possessing high surface areas ($Nb_2O_5 \cdot nH_2O$ and $HCa_2Nb_3O_{10}$).

Introduction

Niobium oxide, Nb_2O_5, has been reported to exist in different polymorphic forms,[1-4] and the phase transformations of niobium oxide strongly depend on the heat treatment. Upon heat treatments between 300 and 1000 °C, amorphous niobium oxide increases in degree of crystallinity and forms more stable Nb_2O_5 phases. Amorphous niobium oxide, $Nb_2O_5 \cdot nH_2O$, possesses distorted NbO_6 octahedra, NbO_7 pentahedra, and NbO_8 hexahedra as structural units.[5] The TT-Nb_2O_5 phase, 300–500 °C, possesses a pseudohexagonal unit cell, with a constitutional defect of an oxygen atom per unit cell, and forms tetragonal and pentagonal bipyramids[1] with six or seven oxygen atoms coordinated to the Nb atom. The T-Nb_2O_5 phase, 700–800 °C, possesses an orthorhombic unit cell and forms distorted tetragonal or pentagonal bipyramids with six or seven oxygen atoms coordinated to the Nb atom. One out of seventeen Nb atoms occupies the interstitial sites between two unit cells and is surrounded by eight oxygen atoms.[6] These polyhedra are joined by corner or edge sharing in the *ab* plane and by corner sharing along the *c* axis. The H-Nb_2O_5 phase, above 1000 °C, is the most thermodynamically stable form of the Nb_2O_5 polymorphs. The structure of H-Nb_2O_5 contains two different sizes of ReO_3-type blocks: 3 × 4 and 3 × 5 blocks composed of corner- or edge-shared NbO_6 octahedra. Only 1 out of 28 Nb sites is a tetrahedron.[7]

The niobium oxide structure can be modified by cation substitution into the crystalline lattice to form different kinds of niobium oxide compounds: perovskite structure,[8-10] layered structure,[11-13] and $Nb_6O_{19}^{8-}$ clusters.[14-16]

(1) Ikeya, T.; Senna, M. *J. Non-Cryst. Solids* **1988**, *105*, 243.
(2) Izumi, F.; Kodama, H. *Z. Anorg. Allg. Chem.* **1978**, *440*, 155.
(3) McConnell, A. A.; Anderson, J. S.; Rao, C. N. R. *Spectrochimica Acta* **1976**, *32A*, 1067.
(4) Weissman, J. G.; Ko, E. I.; Wynblatt, P.; Howe, J. M. *Chem. Mater.* **1989**, *1*, 187.
(5) Aleshina, L. A.; Malnenko, V. P.; Phouphanov, A. D.; Jakovleva, N. M. *J. Non-Csyst. Solids* **1986**, *87*, 350.
(6) Kato, K.; Tamura, S. *Acta Crystallogr.* **1975**, *B31*, 673.
(7) Gatehouse, B. M.; Wadsley, A. *Acta Crystallogr.* **1964**, *17*, 1545.

0897-4756/91/2803-0100$02.50/0